The tomato Nucleotide-Binding Leucine-Rich Repeat (NLR) Immune Receptor I-2 couples DNA-Binding to Nucleotide-Binding Domain Nucleotide Exchange*

Stepan Fenyk[1,2], Christopher H. Dixon[1,2], William H. Gittens[1,2], Philip D. Townsend[1,2], Gary J. Sharples[1,2], Lars-Olof Pålsson[3], Frank L.W. Takken[4,5] and Martin J. Cann[1,2,5]

[1]School of Biological and Biomedical Sciences, [2]Biophysical Sciences Institute, [3]Department of Chemistry, Durham University, South Road, Durham, DH1 3LE, United Kingdom.

[4]Molecular Plant Pathology, Swammerdam Institute for Life Sciences, University of Amsterdam, Science Park 904, 1098 XH, Amsterdam, The Netherlands.

[5]These authors contributed equally to this work

*Running title: *DNA-binding and nucleotide exchange is coupled in I-2*

To whom correspondence should be addressed: Martin J. Cann, School of Biological and Biomedical Sciences, Durham University, South Road, Durham, DH1 3LE, United Kingdom. Phone: +44 (191) 3343985. Fax: +44 (191) 3341201. E-mail: m.j.cann@durham.ac.uk.

Keywords: ATPases associated with diverse cellular activities, Cellular immune response, DNA-binding protein, Nod-like receptor, Plant biochemistry, Nucleotide.

Plant nucleotide-binding leucine-rich repeat (NLR) proteins enable plants to recognise and respond to pathogen attack. Previously, we demonstrated that the Rx1 NLR of potato is able to bind and bend DNA *in vitro.* DNA binding *in situ* requires its genuine activation following pathogen perception. However, it is unknown whether other NLR proteins are also able to bind DNA. Nor is it known how DNA binding relates to the ATPase activity intrinsic to NLR switch function required to immune activation. Here we investigate these issues using a recombinant protein corresponding to the N-terminal coiled-coil and nucleotide-binding domain regions of the I-2 NLR of tomato. Wild type I-2 protein bound nucleic acids with a preference of ssDNA≈dsDNA>ssRNA, which is distinct from Rx1. I-2 induced bending and melting of DNA. Notably, ATP enhanced DNA binding relative to ADP in the wild type protein, the null P-loop mutant K207R, and the autoactive mutant S233F. DNA binding was found to activate the intrinsic ATPase activity of I-2. Since DNA binding by I-2 was decreased in the presence of ADP when compared to ATP, a cyclic mechanism emerges; activated ATP-associated I-2 binds to DNA, which enhances ATP hydrolysis, releasing ADP-bound I-2 from the DNA. Thus DNA-binding is a general property of at least a subset of NLR proteins and NLR activation is directly linked to its activity at DNA.

Plants rely on an innate immune system to ward off pathogens (1-4). Pathogen perception and recognition specificity is typically controlled by NLR-type immune receptors that are capable of perceiving non-self and modified-self molecules inside the host cell. NLRs typically detect strain-specific pathogen effectors or the effect these virulence factors exert on host proteins (3,5,6). NLR proteins are members of the STAND P-loop ATPases of the AAA+ superfamily whose multi-domain structure allows them to function simultaneously as sensor, switch, and response factor (7,8).

Plant NLRs are named after their central NB (Nucleotide Binding) and C-terminal LRR (Leucine Rich Repeat) domains. The N-terminus of a plant NLR is extremely divergent and typically encodes either a CC (Coiled Coil) or TIR (Toll Interleukin Receptor) domain (3). Besides these core domains other domains can be present such as a WRKY, Squamosa promoter binding protein-like (SPL) Heavy-Metal Associated (HMA) or Related to ATX1 (Ratx1) domains that, in conjunction with the LRR, are proposed to aid in effector perception (9-11). The LRR is hypothesised to maintain the NLR protein in a signalling competent, yet auto-inhibited state (12). The central NB domain, also referred to

as the NB-ARC domain due to its homology with APAF1, CED4 and R proteins, is predicted to function as a nucleotide-operated molecular switch controlling the signalling activity of the protein (8,13,14). Biochemical analysis of tomato I-2 and Mi-1, flax M and L6, and barley MLA27 revealed that in the auto-inhibited "off" state the NB-ARC domain is ADP bound (15-17). Upon pathogen recognition ADP is exchanged for ATP permitting the NB-ARC domain to adopt an activated, and structurally distinct, "on" state. Hydrolysis of bound ATP into ADP enables the "off" state to be re-established. There are several lines of supporting evidence for this model. For example, tomato I-2 mutants defective in ATP hydrolysis *in vitro* are auto-active *in vivo* (16). Further, an auto-active flax M mutant preferentially co-purifies with ATP (17). Interestingly, the NLR NB-ARC domain is not necessarily a strict ATPase. The NB sub-domain of rice Os2g_25900, NB-ARC domains of maize Pollen-Signaling Protein (PSiP), and *Arabidopsis* Rpm1 possess a nucleotide phosphatase activity (18). The described phosphatase sequentially removes terminal phosphates from the nucleotide to form the nucleoside in a reaction that remains compatible with the switch model.

How activated plant NLRs trigger immune signalling is a crucial and largely unanswered question. Activation of animal NLRs typically induces multimerisation resulting in the formation of a cytoplasmic signalling scaffold on which partners are activated due to their induced proximity (19). Unlike animal NLRs, no conserved protein binding-partners for plant NLRs have been identified to date that could play an analogous role in downstream signalling. The identified NLR interactors are mostly involved in processes such as NLR protein maturation and folding, nucleo-cytoplasmic shuttling or effector perception (9,12,20). Whereas NLR proteins locate at various subcellular localisations determined by the necessity to intercept effector action at distinct locations, the subcellular localisation from which primary immune signalling is activated is not unambiguously resolved. While some NLRs are confined to a specific subcellular compartment, like the plasma membrane localisation of Rpm1 and the nuclear localisation of RRS1-R (21,22), other NLRs have a more dynamic distribution. For instance tobacco N, barley MLA1 and Mla10, Arabidopsis RPS4 and SNC1 and potato Rx1 show a nuclear-cytoplasmic distribution (22-29). The functional importance of nuclear localisation is emphasised by genetic screens that reveal genes encoding components of the nuclear pore complex to be required for NLR-mediated resistance (30,31). Furthermore, redistribution of MLA10, N, RPS4 and SNC1 from the nucleus to the cytoplasm compromises their immune signalling (24,25,27,31), suggesting that their signalling target resides in the nucleus. Together with the recent notion that many NLRs work in pairs, such as RRS-1/RPS4 and RGA4/RGA5 or require "downstream" or "helper" NLRs such as ADR1, NRG1 or NRC members, this suggests the interesting hypothesis that, even for NLRs not located themselves in the nucleus, the conserved signalling target for NLR signalling might be a nuclear component (32-36).

In line with this hypothesis we recently identified DNA as a molecular target for an activated NLR. We demonstrated that the potato Rx1 NLR possesses an intrinsic DNA binding and melting activity *in vitro* (37). In addition, Rx1 was observed to bend and locally melt dsDNA. DNA binding is mediated by its NB-ARC domain in a manner similar to that of the structurally homologous origin-of-replication binding proteins. An Rx1-DNA interaction in plants was only found upon activation of immune signalling by the Rx-immune elicitor, the CP106 coat protein of PVX virus. No Rx1-DNA interaction was observed in the presence of a PVX virus coat protein variant that is incapable of Rx1 activation, nor was it observed when immune signalling was activated via another NLR protein. This finding raises the exciting possibility that a direct NLR-DNA interaction might be a conserved signalling function of activated NLR proteins. To test this hypothesis we set out to establish whether other NLR proteins are also able to interact with DNA in an activation dependent fashion. Demonstration of a direct DNA interaction by an alternative NLR provides support that this phenomenon is of broad biological relevance. Further, these experiments will allow an appraisal of the mode of interaction and could reveal NLR specific differences in nucleic acid interactions.

The (Immunity to race 2) I-2 NLR protein from tomato, conferring resistance to tomato wilt disease caused by the fungus *Fusarium oxysporum* f.sp. *lycopersici,* is one of the best-studied NLR proteins (16,38). I-2 is a member of the CC-NB-LRR class of plant NLR proteins that consists of an N-terminal CC domain fused to an NB-LRR domain (39). The CC-NB-ARC domain has been heterologously produced in *E. coli* and shown to bind specifically to adenosine nucleotides and to possess ATPase activity *in vitro* (38). Specific amino acid substitutions in its catalytic site, that compromise its ATPase activity, result in a mutant I-2 protein that confers an autoimmune phenotype when expressed *in planta* (16). The I-2 protein

recognises the *Fusarium oxysporum* f.sp. *lycopersici* produced Avr2 protein inside the plant nucleus (40) making I-2 a prime candidate NLR protein to have a nuclear signalling activity like Rx1, MLA, RPS4, RPS5-RRS1, SNC1 and N (23-27,29,41,42).

Here we demonstrate that the I-2 NLR protein of tomato is able to bind, bend, and melt duplex DNA *in vitro*. We find important differences between the Rx1-DNA and I-2-DNA interaction; I-2 shows a nucleic acid-binding specificity distinct from Rx1, but similar to the orphan Os02g_25900 NLR of rice. Furthermore, in contrast to Rx1, the I-2 interaction with DNA is coupled to its nucleotide dependent activation cycle. This directly links DNA interactions with the NLR activation state. We propose that NLR-DNA interactions are a general phenomenon but with NLR-specific differences in the mode of DNA interaction.

EXPERIMENTAL PROCEDURES

Structural Modeling - Protein fold searches using the Phyre[2] protein homology/analogy recognition engine V 2.0 (43) were undertaken using amino acids 175-519 of I-2 and amino acids 197-334 of Os02g_25900 using both normal and intensive modelling modes. Similar structural homology was also detected using the SAM-T08, HMM-based protein structure prediction server (44). Side chain packing and energy minimization was performed using GalaxyRefine (45). Figures were generated using the PyMOL molecular graphics system (46).

Protein expression and purification - Proteins corresponding to I-$2_{1\text{-}519}^{WT}$ and I-$2_{1\text{-}519}^{K207R}$ were generated as described previously (38). The NB sub-domain of Os02g_25900 (amino acids 197-334; R1-NB) was generated as previously described (18). Orc1-1 and Orc1-3 of *S. solfataricus* were expressed and purified as previously described (47).

ATPase assays - ATPase assays were typically performed at 37°C for 30 min with 2.3 μM protein in 50 mM 1,3-bis(tris(hydroxymethyl)methylamino) propane pH 7.5, 10 mM $MgCl_2$, and 5 μM ATP. Reactions were spiked with 0.5 μCi [2,8-^{3}H]-labeled ATP for quantitation. Reactions were spotted onto a silica thin layer chromatography plate with 1 mM ADP to act as both marker and carrier. The plates were developed in isobutanol: 3-methyl-1-butanol: 2-ethoxyethanol: ammonia: H_2O (9:6:18:9:15). Spots were visualized at 256 nm and quantified using an AR-2000 TLC scanner.

Electrophoretic mobility shift assays - The oligonucleotides used for quantitative EMSA are derived from a series of oligonucleotides that enables a comparison of relative DNA-binding affinity to varying DNA topologies independent of DNA sequence (48). The oligonucleotides sequences were 5' TGG GTC AAC GTG GGC AAA GAT GTC CTA GCA ATG TAA TCG TCT ATG ACG TT 3' (SS1; DNA sense-strand), 5' AAC GTC ATA GAC GAT TAC ATT GCT AGG ACA TCT TTG CCC ACG TTG ACC CA 3' (SS2; DNA antisense-strand) and 5' UGG GUC AAC GUG GGC AAA GAU GUC CUA GCA AUG UAA UCG UCU AUG ACG UU 3' (RNA sense-strand) (47). Oligonucleotides were end-labeled with 10 μCi [γ-^{32}P]-ATP using T4 polynucleotide kinase and unincorporated nucleotides removed using Micro Bio-Spin columns (Bio-Rad). Protein and 0.15 nM nucleic acids (oligo 1-ssDNA, annealed oligo 1 and oligo 2-dsDNA, and ssRNA) were incubated in 20 mM Tris-HCl pH 8.0, 60 mM NaCl (unless otherwise stated), 2 mM EDTA, 1 mM DTT, 10% (v/v) glycerol, 0.1 mg/ml BSA for 20 min on ice. Quantitative EMSAs were separated on a native 7% (w/v) polyacrylamide gel. Experiments to assess the role of nucleotides on DNA-binding used binding reactions and gels supplemented with 10 mM $ZnCl_2$ and nucleotide. Polyacrylamide gels were dried and analysed by autoradiography. EMSAs using unlabelled virion DNA were separated using 0.8% (w/v) Tris-acetate-EDTA agarose gels and stained with ethidium bromide. All reported values for K_d represent apparent K_d due to the potential for dissociation of protein-DNA complexes during electrophoresis. Curves were fitted by non-linear regression in GraphPad Prism 6.0.

Fluorescence anisotropy - Changes in anisotropy were measured using a Carey Eclipse Fluorescence Spectrophotometer (Agilent Technologies) fitted with polarizing filters (λ_{em} = 520 nm, λ_{ex} = 495 nm, bandwidth = 5 nm, averaging time = 20 s). Anisotropy was determined using a fluorescein end-labelled oligonucleotide of sequence 5' TGG GTC AAC GTG GGC AAA GA 3' (SS1s; DNA sense-strand) and an unlabelled oligonucleotide of sequence 5' TCT TTG CCC ACG TTG ACC CA 3' (SS2s; DNA antisense-strand) (Eurofins MWG). Oligonucleotides were annealed by heating to 90°C for 3 min in 10 mM Tris pH 8.0, 1 mM EDTA before cooling to room temperature. Protein was titrated into 10 nM labeled oligonucleotide in 6.7 mM Tris-HCl pH 8.0, 3.3 mM sodium acetate, 2 mM EDTA at 25°C. Anisotropy was calculated using WinFLR software (Agilent Technologies).

P_1 nuclease sensitivity - Oligonucleotides for P_1 nuclease sensitivity were 5' CTC AAT ACA ATT GTC TCT GTG TAA ATT TCC TAC GTT TCA TCT GAA AAT CTA GCT ATT AGA GCT TGG TTT A 3' (sense-strand) and 5' TAA ACC AAG CTC TAA TAG CTA GAT TTT CAG ATG AAA CGT AGG AAA TTT ACA CAG AGA CAA TTG TAT TGA G 3' (antisense-strand) and represent the C3/mORB dual site sequence at *oriC2* of *Sulfolobus solfataricus* (49). The sense-strand oligonucleotide was end-labelled with 10 μCi [γ-^{32}P]-ATP as described above and sense and antisense oligonucleotides annealed as required. Reactions were performed in 20 μl volumes containing 20 mM Tris-acetate pH 7.5, 10 mM magnesium acetate, 100 mM NaCl, 0.15 nM oligonucleotide, and 1.5 μM protein. Protein was allowed to bind for 10 min at 37°C. P_1 nuclease was added to a final concentration of 0.01-0.1 U μl^{-1} and incubated for a further 20-60 min at 37°C. Reactions were terminated with 5 μl 100 mM Tris-HCl pH 8.0, 2.5% (w/v) SDS, 100 mM EDTA, 10 U μl^{-1} proteinase K. 5 μl of loading buffer (97.5% (v/v) formamide, 10 mM EDTA, 0.3% (w/v), 0.3% bromophenol blue) was added and reactions electrophoresed on a 15% (w/v) polyacrylamide gel containing 8 M urea. Polyacrylamide gels were dried and analysed by autoradiography. The BSA and ORC controls lanes presented in Figure 4 are identical to those previously published as the I-2 and Rx1 samples have been analysed side-by-side (37).

Steady-state FRET in vitro - Synthetic oligonucleotides, unlabeled or end-labeled with fluorescein or tetramethylrhodamine (TAMRA), were purchased from Eurofins MWG. The oligonucleotides used were 5' TGG GTC AAC GTG GGC AAA GA 3' (SS1s; DNA sense-strand) and 5' TCT TTG CCC ACG TTG ACC CA 3' (SS2s; DNA antisense-strand). Oligonucleotides were annealed by heating to 90°C for 3 min in 10 mM Tris pH 8.0, 1 mM EDTA before cooling to room temperature. Steady-state FRET was measured using a Perkin-Elmer LS 55 Fluorescence Spectrometer at room temperature in a final volume of 50 μL with 50 nM DNA. Measurements used 1.5 μM protein and were incubated for 10 min at room temperature before scanning. A bandwidth of 5 nm was used for both excitation and emission wavelengths. Donor (fluorescein) was excited at 494 nm and emission spectra collected from 490-650 nm. Acceptor (TAMRA) was directly excited at 558 nm and emission spectra collected from 558-650 nm. Spectra were collected for both donor and donor-acceptor labeled double-stranded DNA and FRET calculated from the increase in acceptor emission using the $ratio_A$ method (50). $Ratio_A$ was used to calculate energy transfer efficiency (E) using the equation $E=(\varepsilon_A[558]/ =\varepsilon_D[494]) \times ratio_A - (\varepsilon_A[494]/ =\varepsilon_A[558])$ where $\varepsilon_A[\lambda]$ and $\varepsilon_D[\lambda]$ are the acceptor and donor extinction coefficients provided by the supplier. Donor-acceptor distances (R) were calculated using the equation $E=R_0^6/(R_0^6+R^6)$ and a calculated Förster distance (R_0) of 49.99 Å. The induced bend angle (θ_T) was calculated using a single-point bend model.

Time-resolved FRET in vitro – Oligonucleotides were as for steady-state FRET *in vitro* and annealed in the same manner. Strands were annealed by heating to 90°C for 3 min in 10 mM Tris pH 8.0, 1 mM EDTA before cooling to room temperature. Measurements used 1.5 μM protein with 50 nM DNA in the presence of 60 mM NaCl and were incubated for 10 min at room temperature before analysis. Time-resolved FRET was assessed using the Time-Correlated, Single Photon Counting (TCSPC) technique. The excitation source was a Picoquant pulsed diode laser LDH-P-C-485 (excitation wavelength 485 nm, 70 ps pulse FWHM at 20 MHz). Fluorescence was detected using an avalanche photodiode (Id Quantique 100-50) linked to a Becker and Hickl SPC 130 TCSPC module. An instrument response function of ~200 ps was measured from Rayleigh scattered light. Fluorescence decays were collected for both donor and donor-acceptor labelled double-stranded DNA with or without protein using band pass filter detection of the donor emission and at magic angle polarization.

Data was analyzed by the Grinvald-Steinberg method (51) to obtain the fluorescence lifetime for the donor and acceptor (τ_{DA}) and donor only (τ_D) labelled oligonucleotides. The data was fitted to a sum of exponentials using an iterative least squares re-convolution procedure with the optical/electrical excitation profile to produce a bi-exponential decay containing two lifetimes. This profile was obtained from a slide covered with Silica ludox particles, which provides an instant scatter of the excitation pulse. This data-fitting method provided more accuracy in the determination of shorter lifetimes than calculating a single average lifetime. Efficiencies of energy transfer were calculated from time-resolved FRET according to $E=1-(\tau_{DA}/\tau_D)$. Energy transfer efficiencies in the lifetime analysis were higher than those from steady-state experiments as previously observed (52-54).

Donor-acceptor distances (R) were calculated using the equation $E=R_0^6/(R_0^6+R^6)$ and a calculated Förster distance (R_0) of 49.99 Å. The total length of the oligonucleotide with linkers and fluorescent dyes, at maximum extension, was calculated as 81.1 Å. The induced bend angle (θ_T) was calculated using a single-point bend model.

Statistical analysis - Error bars represent the standard error of the mean with the number of replicates as indicated in the legend. Statistical comparisons (p values) for data that passes a test for normality (D'Agostino & Pearson omnibus normality test and Shapiro-Wilk normality test) were obtained from one-way ANOVA with the indicated post-hoc test. Statistical comparisons (p values) for data that does not pass a test for normality were obtained from a Kruskal-Wallis test with post-hoc multiple comparisons test. P values in statistical comparisons are indicated in figures through letters and indicate compared data sets as described in the figure legends.

RESULTS

I-2 binds nucleic acids in vitro – The NB-ARC domain of Rx1 (amino acids 143-488) has significant homology with the Cdc6/Orc1 proteins of *Pyrobaculum aerophilum* (PDB 1FNN) and of *Aeropyrum pernix* (PDB 2V1U) in complex with DNA (37). We therefore investigated whether there is a similar structural homology in I-2. Amino acids 175-519 of I-2, encompassing the NB-ARC domain, were analysed using the Phyre[2] protein fold recognition engine and the expected close matches with the pro-apoptotic proteins CED-4 (PDB 2A5Y) and Apaf-1 (PDB 1Z6T) were recovered to 100% confidence (55,56). Like Rx1, high scoring matches (>99% confidence) were also obtained with the Cdc6/Orc1 protein family members. Residues in the NB sub-domain and tandem ARC domains were conserved between Cdc6/Orc1 of *Aeropyrum pernix* and I-2 (29.7% similarity and 9.9% identity). Both the N-terminal NB (amino acids 22-193) and C-terminal ARC domains (amino acids 194-388) in Cdc6/Orc1 contact DNA, inducing deformation of the double helix (47,49), and the modelled tertiary structure of I-2 closely matched that of Cdc6/Orc1 (Figure 1A). Structural modelling therefore suggests that the NB-ARC domain of I-2 could contact DNA in a manner similar to that of Cdc6/Orc1 and as hypothesized for Rx1. We therefore investigated whether I-2 is also a DNA-binding protein.

A possible direct I-2-DNA interaction was investigated through *in vitro* experiments. EMSA using nucleic acid fragments of >5 kb derived from circular bacteriophage ϕX174 (57) represents a standard methodology to qualitatively assess interactions between a protein and either single-stranded (ss) or double-stranded (ds) DNA with identical sequences. EMSAs were performed using recombinant wild-type I-2 protein ($I\text{-}2_{1\text{-}519}^{WT}$), encompassing the CC-NB-ARC region, but lacking the LRR (Figure 1B). EMSA experiments performed with $I\text{-}2_{1\text{-}519}^{WT}$ showed a direct association with both ssDNA and dsDNA, producing an upward shift in the migration of the nucleic acids similar to that of Rx1 and other unrelated DNA-binding proteins (Figure 1C) (18,58). I-2 is therefore able to interact with both ssDNA and dsDNA in a sequence independent manner.

The I-2-DNA interaction was relatively stable as it could be visualized after gel electrophoresis (Figure 1C). Nevertheless, while EMSA using circular bacteriophage ϕX174 DNA is a useful method to qualitatively assess the interaction, it does not enable robust quantification of the affinity of I-2 for nucleic acids. We therefore shifted to EMSAs using small synthetic oligonucleotides to quantify I-2-nucleic acid interactions (59). EMSA with oligonucleotides provides more robust band shifts on EMSA due to their lower molecular mass.

The affinity of $I\text{-}2_{1\text{-}519}^{WT}$ was assessed using ^{32}P-labeled synthetic oligonucleotides whose sequences were unrelated to that of bacteriophage ϕX174 DNA. $I\text{-}2_{1\text{-}519}^{WT}$ showed equivalent affinities for ssDNA and dsDNA but a reduced affinity for ssRNA (Figure 2A, Table 1). The ordering of affinities of $I\text{-}2_{1\text{-}519}^{WT}$ for nucleic acid (ssDNA≈dsDNA>ssRNA) is distinct to those of Rx1 (ssDNA>ssRNA>dsDNA) implying that different NLRs can have distinct nucleic acid-binding properties *in vitro*. One caveat to this observation is that I-2 is a refolded recombinant protein. Hence, its altered nucleic acid specificity might be a reflection of its refolded status. We therefore investigated the nucleic acid binding specificity of a natively folded NB-ARC subdomain.

We were unable to produce the individual NB or NB-ARC subdomains of I-2 in *E. coli* and therefore shifted to the isolated NB sub-domain of an I-2 homolog, the orphan NB-LRR protein Os02g_25900 (R1-NB). R1-NB was selected for analysis as it has been previously demonstrated to be readily expressed as a natively folded protein in *E. coli* (18). R1-NB therefore avoids the criticism that its activity might be affected by the *in vitro* refolding procedure that could result in a subfraction of potentially mis- or unfolded protein. Furthermore, structural modelling demonstrated a close structural

similarity between the NB domains of R1-NB and that of I-2 (Figure 2B). Like I-2_{1-519}^{WT} R1-NB bound both circular bacteriophage ϕX174 ssDNA and dsDNA in a sequence independent fashion (Figure 2C). R1-NB interacted with a variety of oligonucleotides with an ordering of affinities for nucleic acids of ssDNA≈dsDNA>ssRNA (Figure 2D, Table 1). The ranking for R1-NB is similar to that observed for I-2_{1-519}^{WT} with a clear preference for binding DNA over RNA. We hence conclude that the nucleic acid affinities for I-2 are likely a reflection of its genuine biochemistry and not an artefact of refolding the recombinant protein.

The P-loop mutation K207R of I-2 (I-2_{1-519}^{K207R}) reduces the K_M for ATP *in vitro* and confers a loss of function phenotype *in vivo* (38). We therefore set out to test whether the I-2 K207R mutant shows a similar distinct pattern of interaction when compared to the wild type protein. We first compared the affinity of I-2_{1-519}^{WT} and I-2_{1-519}^{K207R} for dsDNA. Using an EMSA assay the affinities of I-2_{1-519}^{WT} and I-2_{1-519}^{K207R} for dsDNA were largely indistinguishable (Figure 3A). However, when the affinity of I-2_{1-519}^{WT} and I-2_{1-519}^{K207R} was compared using fluorescence anisotropy the affinity of I-2_{1-519}^{WT} for dsDNA was significantly greater than that of I-2_{1-519}^{K207R} (Figure 3B, Table 1). Affinities measured by anisotropy depend not only upon the mass of a protein-DNA complex at a given molar ratio, but also on its globular structure. EMSA therefore suggests that the binding constants of I-2_{1-519}^{WT} and I-2_{1-519}^{K207R} are very similar but anisotropy reveals that the overall shape of the protein complex on DNA might be different. Together these data indicate that, like Rx1, I-2 and R1 interact with nucleic acids, but that the affinities for different nucleic acids vary for the different NLRs. Further, the structure of the NLR-DNA complex formed in I-2 depends on the presence of an intact P-loop.

I-2 deforms DNA – The Cdc6/Orc1 family proteins substantially deform origin DNA by bending it with angles of 35° and 20° respectively, thereby inducing localized melting of the double helix (47,49,60). The Rx1 protein is also able to bend dsDNA through an angle of 42° (37). We therefore investigated whether I-2 is able to deform dsDNA in a similar fashion. We examined DNA distortion by steady-state FRET using two-sided end-labeled dsDNA (61). DNA distortion was evident by an increase in FRET acceptor emission in the presence of I-2_{1-519}^{WT} or I-2_{1-519}^{K207R} when compared to the mock (no protein) or to a control protein (BSA) (Figure 4A). Energy transfer efficiency correlates with the distance between fluorophores and was found to increase in the presence of I-2_{1-519}^{WT} or I-2_{1-519}^{K207R}. The change in efficiency can be used to calculate their distances and revealed that I-2_{1-519}^{WT} and I-2_{1-519}^{K207R} induced bend angles (θ_T) of 21.8-23.9 ° and 22.1-23.1°, respectively (values represent a range of ±1 S.E.M. from the mean). We next measured the fluorescence lifetime, which represents an intrinsic property of the fluorophore that is independent of concentration, photobleaching and light scattering, as an alternative method to measure DNA distortion through a FRET process. The decrease in fluorescent donor lifetime can only be rationalized due to increased energy transfer from donor to the acceptor. Together with the data from steady-state analysis these data both show increased energy transfer efficiency from donor to acceptor in the presence of I-2_{1-519}^{WT} or I-2_{1-519}^{K207R} (Figure 4B). The recorded fluorescence lifetimes correspond to θ_T values for I-2_{1-519}^{WT} and I-2_{1-519}^{K207R} of 29.7-36.7° and 29.6-35.1° respectively (values represent a range of ±1 S.E.M. from the mean). In conclusion, I-2_{1-519} distorts DNA like Cdc6/Orc1 and R1. However, the bend angle induced by I-2, as measured by two independent methods, is substantially lower than that induced by Rx1, indicating a similar, yet distinct mode of action.

The Orc1 protein of *Aeropyrum pernix* (70) and Rx1 also induce local DNA distortion upon binding. The P_1 nuclease can be used to detect distortion specific ssDNA in the presence of the bending proteins (37,60,62). We therefore examined the sensitivity of dsDNA oligonucleotides to the ssDNA-specific P_1 nuclease in the presence of I-2_{1-519}. As expected, ssDNA was significantly degraded (positive control) whereas dsDNA, in the presence of BSA (negative control), was largely resistant to P_1 nuclease activity (Figure 4C). dsDNA was more sensitive to P_1 nuclease in the presence of either I-2_{1-519}^{WT} or the mutant I-2_{1-519}^{K207R}, showing that both proteins can melt dsDNA. The P_1 sensitivity of dsDNA in the presence of Orc1-1/Orc1-3 was indistinguishable from that of dsDNA in the presence of I-2_{1-519} supporting the interpretation that I-2, similar to Rx1, can cause local dsDNA melting (Figure 4C). In conclusion, I-2 is able to bend DNA and provoke localized DNA melting. As the pattern of DNA distortion induced by I-2 is indistinguishable between I-2_{1-519}^{WT} and the mutant I-2_{1-519}^{K207R}, the difference in the nature of the protein-DNA complex is not at the level of melting the DNA.

The I-2-DNA interaction is coupled to the nucleotide binding state and activity of the P-loop – The findings on DNA interaction and distortion seem to indicate that the difference between I-2_{1-}

$_{519}^{WT}$ and the mutant I-2_{1-519}^{K207R} is related to the conformational state of the protein (Figure 3B) and not DNA melting (Figure 4C). We therefore sought independent evidence to understand the relationship between the nucleotide occupancy and ATPase activity of the P-loop in I-2 (compromised in I-2_{1-519}^{K207R}) and DNA binding. In the 'switch' model for plant NLR activation, binding of ATP to the NB-ARC domain establishes the 'on' state while hydrolysis of ATP to ADP restores the 'off' state (13). An intact P-loop is essential for nucleotide binding and mutations in this motif typically result in loss-of-function alleles (13). We therefore investigated the relationship between P-loop-dependent ATPase activity and DNA-binding. The CC-NB-ARC domain of I-2 has a very low intrinsic ATPase activity *in vitro*. Interestingly, the ATPase activity of I-2_{1-519}^{WT} was increased 2-fold in the presence of DNA (Figure 5A). Although I-2_{1-519}^{K207R} has a reduced ATPase activity, reflecting its lowered K_M for ATP, its enzymatic activity was also stimulated 2-fold by DNA.

Next, we tested the reciprocal relationship and examined whether nucleotides influence DNA binding by I-2_{1-519}. To be able to monitor either increased- or reduced binding capacity an I-2_{1-519} protein concentration was used that gives approximately 50% of maximal DNA binding. The ratio of I-2_{1-519}^{WT} bound to DNA in the presence of 5 μM ATP (giving about 70% nucleotide occupancy for I-2_{1-519}^{WT} (16)) compared to DNA-bound I-2_{1-519}^{WT} in the absence of nucleotides was approximately unity (Figure 5B). In contrast, the ratio of I-2_{1-519}^{WT} bound to DNA in the presence of 5 μM ADP was approximately 0.65 as compared to that in the presence of ATP or in the absence of nucleotides demonstrating a reduced binding of the I-2-ADP complex. Binding of I-2_{1-519}^{WT} to DNA in the presence of the non-hydrolysable ATP analogue, adenosine 5'-(β, γ-imido)triphosphate, was indistinguishable from DNA binding in the presence of ATP ruling out that the enhanced binding, compared to that measured in the presence of ADP is due to hydrolysis of ATP. The influence of nucleotides on I-2_{1-519}^{K207R} DNA binding was the same as that for I-2_{1-519}^{WT}. Since K207R is a K_M mutation that likely effects co-ordination of the ATP β-PO_4^{2-} it is not surprising that this mutant shows a similar response to the nucleotides. As the ATP and 'no nucleotide'-bound states appear equivalent in this assay, it was also to be expected that this mutant behaved similarly to the wild type despite its lowered K_M for ATP.

To provide further evidence that the difference between the DNA-binding ability of the ATP and ADP-bound states is not due to changes in nucleotide handling we investigated an additional I-2 mutant. The S233F mutant is autoactive *in vivo* due to its reduced ATP hydrolysis rate while it has an affinity for ATP equivalent to wild type (16). Binding of I-2_{1-519}^{S233F} to dsDNA was indistinguishable from I-2_{1-519}^{WT} (Figure 5C). We found that for I-2_{1-519}^{S233F}, similar to wild type I-2, DNA binding in the presence of 5 μM ADP was only 61±7% (S.D.) of that in the presence of 5 μM ATP. This observation further supports our hypothesis that DNA-binding by I-2 is enhanced by ATP relative to ADP, and that this change cannot be attributed to differences in nucleotide handling by the different proteins.

Together these results indicate that the intrinsic ATPase activity of I-2 is enhanced in the presence of DNA. This converts the ATP-bound state into the ADP-bound conformation with a consequent increased likelihood for release from DNA.

DISCUSSION

Immune responses induced by NLR immune receptors are broadly conserved (63), suggesting a common signaling network that might be activated via a conserved mechanism. Existing *in vitro*, *in vivo* and bioinformatics data identify the NB-ARC domain as the most conserved domain in NLR proteins. The NB-ARC domain functions as a molecular switch regulating NLR activity. Its conservation makes the NB-ARC domain also a prime candidate to be involved in activating the downstream signalling process. The NB-ARC domain of the potato Rx1 NLR protein was shown to possess an intrinsic DNA-binding activity that is activated *in situ* only upon triggering the cellular immune response by admission of the pathogen-derived elicitor (37). Here we demonstrate that both R1 of rice and I-2 of tomato are also able to interact with nucleic acids *in vitro*. This study, therefore, establishes nucleic acid interactions as central to the biochemistry for at least a subset of NLR proteins. The observed specificity for ssDNA, dsDNA and RNA for these proteins revealed subtle differences in their abilities to interact with nucleic acids. The functional relevance of these differences awaits future elucidation.

I-2 shares many biochemical properties with Rx1 and the Cdc6/Orc1 family of DNA-binding proteins. I-2 was observed to bind both ssDNA and dsDNA similar to ORC of *Saccharomyces cerevisiae* and Rx1 (37,64). Based upon the Cdc6/Orc1 homology with NLR proteins, and the DNA-binding characteristics of the isolated R1 NB

domain (Figure 2b), it is most likely that this domain is also the site of DNA binding in the I-$2_{1\text{-}519}$ protein, although a role for the CC domain cannot be formally excluded. Unfortunately it was not possible to generate truncated I-2 protein lacking the CC domain to test this hypothesis. Eukaryotic ORCs and Rx1 lack DNA sequence specificity *in vitro* and this property is also shared with I-2 (88,89). Superficially, therefore, I-2 biochemistry and ability to interact with nucleotides appears similar to Rx1. Similar to Rx1, the I-2 protein used for analysis is lacking its LRR domain region. The absence of a domain resembling the LRR in Cdc6/Orc1 proteins validates the use of this truncated protein in assessing DNA binding in NLR proteins. However, we cannot exclude the possibility that the LRR might influence the affinity of the NB-ARC region for DNA through constraints placed on relative domain orientations. These experiments are an important future target but which first require the synthesis of significant amounts of full-length NLR protein, currently a considerable technical challenge.

A number of crucial differences, however, between the biochemistry of Rx1 and I-2 are observed. First, Rx1 and I-2 show divergent specificity for different nucleic acid species. Rx1 has a higher affinity for single-stranded nucleic acids (ssDNA and RNA) over double-stranded nucleic acids while I-2 has a higher affinity for dsDNA over RNA. The significance of this for the respective NLRs will await future functional characterization. Both Rx1 and I-2 distort dsDNA but to differing extents. The bend angle introduced into DNA by I-2 (22 to 33°) is substantially less than that introduced by Rx1 (42°) but of a similar magnitude as that introduced by Orc1-1/Orc1-3 of *Sulfolobus solfataricus* (20°) and ORC1 of *Aeropyrum pernix* (35°) (37,47,49). The most noticeable difference between Rx1 and I-2, however, is that I-2 allows us to make a coupling between its P-loop - required for the switch function - and DNA binding. In contrast to Rx1, I-2 has a measurable ATPase activity, which we found to be stimulated by DNA (Figure 5a). Furthermore, (non-hydrolysable) ATP was demonstrated to promote I-2 binding to DNA relative to the ADP-bound state. This observed property is consistent with the switch hypothesis for NB-ARC domain activation stating that the "open" ATP-bound state is the active state triggering immune signalling, whereas the "closed" ADP-bound conformation corresponds to the autoinhibited state (8). Increased DNA binding in the presence of ATP and a non-hydrolysable ATP analogue, when compared to ADP, suggests that DNA binding is stimulated in response to NLR activation upon effector recognition. That ATP-bound and non-nucleotide bound I-2 show similar binding to DNA suggests that the structure of the empty protein resembles that of the activated state and differs from that the "closed" ADP bound confirmation. Incubation with DNA stimulates the ATPase activity of I-2 suggesting that DNA binding is a self-limiting process and it is tempting to speculate that DNA binding and release is a cyclic process triggered by the presence of the effector. A similar cyclic mechanism, allowing multiple rounds of elicitor recognition providing a means for signal amplification, has been proposed before for Rx and was based on interaction studies of the CC-NB-ARC and LRR domains (65). Further study is required to assess the significance and generality of these findings for other NLRs.

Additional evidence linking coupling of the activation state and switch function of the NB-ARC to DNA binding comes from the analysis of an I-2 P-loop mutant. Wild type I-2 and a variant with a defective P-loop have a similar affinity for double-stranded DNA as assessed by EMSA. However, measurements using fluorescence anisotropy reveal a reduced affinity for the P-loop mutant. These data suggest an overall different shape for the protein-DNA complex for the wild type and P-loop mutant proteins. This difference is not due to alternations in conformation of the bound DNA as the observed pattern of DNA distortion, measured through DNA bending and melting, is identical in both cases. It is reasonable to assume, therefore, that the difference in topology is attributed to the protein. In support of this hypothesis, equivalent mutations in the NB domain of Cdc6 have been shown to affect its ability to interact with other proteins and form complexes at dsDNA (66,67). It is formally possible that anisotropy, but not EMSA, detects an I-2 complex that forms for the wild type, but not the mutant protein. Such a complex could result in a higher observed anisotropy. These observations provide insight into the molecular mechanism for how P-loop mutations, commonly used to investigate the role of NLR switch function in immunity, might exert their activity. NLR variants with P-loop modifications, such as the I-2 K207R mutant, showing a decreased K_M [ATP] are defective in immune activation. At cellular [ATP], this defect may not necessarily contribute to decreased ATP binding but may be a reflection of an altered conformational state that could influence trafficking (29) or its activity at DNA (66,67). Unfortunately, chimeric fusions of I-2 with GFP are non-functional, so we cannot use microscopic methods to investigate the effect P-loop mutants have on I-2 mediated DNA

binding *in planta* in relation to immune signalling (37).

In summary, we have identified a DNA-binding and distorting activity in the I-2 protein *in vitro*. This establishes nucleic acid binding as a conserved biochemical feature for at least a subset of plant NLR proteins (I-2, R1, Rx1 and PSiP). A further conserved feature of these NLR proteins in DNA manipulation is through bending and melting of the double helix. We further establish that individual NLR proteins distinctively differ in the interactions with various nucleotide topologies (ssDNA, dsDNA and RNA) that might arise from their functional diversity. DNA binding in I-2 is directly linked to the switch function of its central NB-ARC domain thus directly linking activity at DNA to known biochemical requirements for NLR activation.

.

CONFLICT OF INTEREST STATEMENT

The authors declare that they have no conflicts of interest with the contents of this article.

AUTHOR CONTRIBUTIONS

SF, PDT, CHD, and WHG performed the experiments. SF, PDT, CHD, WHG, GJS, LOP, FLWT and MJC analysed the data. GJS, LOP, FLWT and MJC conceived the experiments. MJC and FLWT conceived the overall project and wrote the manuscript. All authors reviewed the results and approved the final version of the manuscript.

REFERENCES

1. Dangl, J. L., and Jones, J. D. (2001) Plant pathogens and integrated defence responses to infection. *Nature* **411**, 826-833
2. Jones, J. D., and Dangl, J. L. (2006) The plant immune system. *Nature* **444**, 323-329
3. Maekawa, T., Kufer, T. A., and Schulze-Lefert, P. (2011) NLR functions in plant and animal immune systems: so far and yet so close. *Nat Immunol* **12**, 817-826
4. Medzhitov, R. (2007) Recognition of microorganisms and activation of the immune response. *Nature* **449**, 819-826
5. Eitas, T. K., and Dangl, J. L. (2010) NB-LRR proteins: pairs, pieces, perception, partners, and pathways. *Curr Opin Plant Biol* **13**, 472-477
6. Staskawicz, B. J., Mudgett, M. B., Dangl, J. L., and Galan, J. E. (2001) Common and contrasting themes of plant and animal diseases. *Science* **292**, 2285-2289
7. Leipe, D. D., Koonin, E. V., and Aravind, L. (2004) STAND, a class of P-loop NTPases including animal and plant regulators of programmed cell death: multiple, complex domain architectures, unusual phyletic patterns, and evolution by horizontal gene transfer. *J Mol Biol* **343**, 1-28
8. Takken, F. L., and Tameling, W. I. (2009) To nibble at plant resistance proteins. *Science* **324**, 744-746
9. Cesari, S., Bernoux, M., Moncuquet, P., Kroj, T., and Dodds, P. N. (2014) A novel conserved mechanism for plant NLR protein pairs: the "integrated decoy" hypothesis. *Front Plant Sci* **5**, 606
10. Nishimura, M. T., Monteiro, F., and Dangl, J. L. (2015) Treasure your exceptions: unusual domains in immune receptors reveal host virulence targets. *Cell* **161**, 957-960
11. Maqbool, A., Saitoh, H., Franceschetti, M., Stevenson, C., Uemura, A., Kanzaki, H., Kamoun, S., Terauchi, R., and Banfield, M. J. (2015) Structural basis of pathogen recognition by an integrated HMA domain in a plant NLR immune receptor. *eLife* **4**
12. Lukasik, E., and Takken, F. L. (2009) STANDing strong, resistance proteins instigators of plant defence. *Curr Opin Plant Biol* **12**, 427-436
13. Takken, F. L., Albrecht, M., and Tameling, W. I. (2006) Resistance proteins: molecular switches of plant defence. *Curr Opin Plant Biol* **9**, 383-390
14. van der Biezen, E. A., and Jones, J. D. G. (1998) The NB-ARC domain: a novel signalling motif shared by plant resistance gene products and regulators of cell death in animals. *Curr. Biol.* **8**, R226-227
15. Maekawa, T., Cheng, W., Spiridon, L. N., Toller, A., Lukasik, E., Saijo, Y., Liu, P., Shen, Q. H., Micluta, M. A., Somssich, I. E., Takken, F. L., Petrescu, A. J., Chai, J., and Schulze-Lefert, P. (2011) Coiled-coil domain-dependent homodimerization of intracellular barley immune receptors defines a minimal functional module for triggering cell death. *Cell Host Microbe* **9**, 187-199
16. Tameling, W. I., Vossen, J. H., Albrecht, M., Lengauer, T., Berden, J. A., Haring, M. A., Cornelissen, B. J., and Takken, F. L. (2006) Mutations in the NB-ARC domain of I-2 that impair ATP hydrolysis cause autoactivation. *Plant Physiol* **140**, 1233-1245
17. Williams, S. J., Sornaraj, P., Decourcy-Ireland, E., Menz, R. I., Kobe, B., Ellis, J., Dodds, P., and Anderson, P. A. (2011) An autoactive mutant of the M flax rust resistance protein has a preference for binding ATP, while wild-type M protein has a preference for binding ADP. *Mol Plant Microbe Interact* **24**, 897-906
18. Fenyk, S., Campillo Ade, S., Pohl, E., Hussey, P. J., and Cann, M. J. (2012) A nucleotide phosphatase activity in the nucleotide binding domain of an orphan resistance protein from rice. *J Biol Chem* **287**, 4023-4032

19. von Moltke, J., Ayres, J. S., Kofoed, E. M., Chavarria-Smith, J., and Vance, R. E. (2013) Recognition of bacteria by inflammasomes. *Annu Rev Immunol* **31**, 73-106
20. Griebel, T., Maekawa, T., and Parker, J. E. (2014) NOD-like receptor cooperativity in effector-triggered immunity. *Trends Immunol* **35**, 562-570
21. Gao, Z., Chung, E. H., Eitas, T. K., and Dangl, J. L. (2012) Plant intracellular innate immune receptor Resistance to Pseudomonas syringae pv. maculicola 1 (RPM1) is activated at, and functions on, the plasma membrane. *Proc Natl Acad Sci U S A* **108**, 7619-7624
22. Deslandes, L., Olivier, J., Peeters, N., Feng, D. X., Khounlotham, M., Boucher, C., Somssich, I., Genin, S., and Marco, Y. (2003) Physical interaction between RRS1-R, a protein conferring resistance to bacterial wilt, and PopP2, a type III effector targeted to the plant nucleus. *Proc Natl Acad Sci USA* **100**, 8024-8029
23. Bai, S., Liu, J., Chang, C., Zhang, L., Maekawa, T., Wang, Q., Xiao, W., Liu, Y., Chai, J., Takken, F. L., Schulze-Lefert, P., and Shen, Q. H. (2012) Structure-function analysis of barley NLR immune receptor MLA10 reveals its cell compartment specific activity in cell death and disease resistance. *PLoS pathogens* **8**, e1002752
24. Shen, Q. H., Saijo, Y., Mauch, S., Biskup, C., Bieri, S., Keller, B., Seki, H., Ulker, B., Somssich, I. E., and Schulze-Lefert, P. (2007) Nuclear activity of MLA immune receptors links isolate-specific and basal disease-resistance responses. *Science* **315**, 1098-1103
25. Wirthmueller, L., Zhang, Y., Jones, J. D., and Parker, J. E. (2007) Nuclear accumulation of the Arabidopsis immune receptor RPS4 is necessary for triggering EDS1-dependent defense. *Curr Biol* **17**, 2023-2029
26. Zhu, Z., Xu, F., Zhang, Y., Cheng, Y. T., Wiermer, M., and Li, X. (2010) Arabidopsis resistance protein SNC1 activates immune responses through association with a transcriptional corepressor. *Proc Natl Acad Sci USA* **107**, 13960-13965
27. Burch-Smith, T. M., Schiff, M., Caplan, J. L., Tsao, J., Czymmek, K., and Dinesh-Kumar, S. P. (2007) A novel role for the TIR domain in association with pathogen-derived elicitors. *PLoS Biol* **5**, e68
28. Caplan, J. L., Mamillapalli, P., Burch-Smith, T. M., Czymmek, K., and Dinesh-Kumar, S. P. (2008) Chloroplastic protein NRIP1 mediates innate immune receptor recognition of a viral effector. *Cell* **132**, 449-462
29. Slootweg, E., Roosien, J., Spiridon, L. N., Petrescu, A. J., Tameling, W., Joosten, M., Pomp, R., van Schaik, C., Dees, R., Borst, J. W., Smant, G., Schots, A., Bakker, J., and Goverse, A. (2010) Nucleocytoplasmic distribution is required for activation of resistance by the potato NB-LRR receptor Rx1 and is balanced by its functional domains. *Plant Cell* **22**, 4195-4215
30. Wiermer, M., Germain, H., Cheng, Y. T., Garcia, A. V., Parker, J. E., and Li, X. (2010) Nucleoporin MOS7/Nup88 contributes to plant immunity and nuclear accumulation of defense regulators. *Nucleus* **1**, 332-336
31. Cheng, Y. T., Germain, H., Wiermer, M., Bi, D., Xu, F., Garcia, A. V., Wirthmueller, L., Despres, C., Parker, J. E., Zhang, Y., and Li, X. (2009) Nuclear pore complex component MOS7/Nup88 is required for innate immunity and nuclear accumulation of defense regulators in Arabidopsis. *Plant Cell* **21**, 2503-2516
32. Bonardi, V., Tang, S. J., Stallmann, A., Roberts, M., Cherkis, K., and Dangl, J. L. (2011) Expanded functions for a family of plant intracellular immune receptors beyond specific recognition of pathogen effectors. *Proc Natl Acad Sci USA* **108**, 16463-16468
33. Gabriels, S. H., Vossen, J. H., Ekengren, S. K., van Ooijen, G., Abd-El-Haliem, A. M., van den Berg, G. C., Rainey, D. Y., Martin, G. B., Takken, F. L., de Wit, P. J., and Joosten, M. H. (2007) An NB-LRR protein required for HR signalling mediated by both extra- and intracellular resistance proteins. *Plant J* **50**, 14-28
34. Cesari, S., Thilliez, G., Ribot, C., Chalvon, V., Michel, C., Jauneau, A., Rivas, S., Alaux, L., Kanzaki, H., Okuyama, Y., Morel, J. B., Fournier, E., Tharreau, D., Terauchi, R., and Kroj, T. (2013) The rice resistance protein pair RGA4/RGA5 recognizes the Magnaporthe oryzae effectors AVR-Pia and AVR1-CO39 by direct binding. *Plant Cell* **25**, 1463-1481
35. Cesari, S., Kanzaki, H., Fujiwara, T., Bernoux, M., Chalvon, V., Kawano, Y., Shimamoto, K., Dodds, P., Terauchi, R., and Kroj, T. (2014) The NB-LRR proteins RGA4 and RGA5 interact functionally and physically to confer disease resistance. *EMBO J* **33**, 1941-1959

36. Le Roux, C., Huet, G., Jauneau, A., Camborde, L., Tremousaygue, D., Kraut, A., Zhou, B., Levaillant, M., Adachi, H., Yoshioka, H., Raffaele, S., Berthome, R., Coute, Y., Parker, J. E., and Deslandes, L. (2015) A receptor pair with an integrated decoy converts pathogen disabling of transcription factors to immunity. *Cell* **161**, 1074-1088
37. Fenyk, S., Townsend, P. D., Dixon, C. H., Spies, G. B., de San Eustaquio Campillo, A., Slootweg, E. J., Westerhof, L. B., Gawehns, F. K., Knight, M. R., Sharples, G. J., Goverse, A., Palsson, L. O., Takken, F. L., and Cann, M. J. (2015) The Potato Nucleotide-Binding Leucine-Rich Repeat (NLR) Immune Receptor Rx1 is a Pathogen Dependent DNA-Deforming Protein. *J Biol Chem* **290**, 24945-24960
38. Tameling, W. I., Elzinga, S. D., Darmin, P. S., Vossen, J. H., Takken, F. L., Haring, M. A., and Cornelissen, B. J. (2002) The tomato R gene products I-2 and MI-1 are functional ATP binding proteins with ATPase activity. *Plant Cell* **14**, 2929-2939
39. Simons, G., Groenendijk, J., Wijbrandi, J., Reijans, M., Groenen, J., Diergaarde, P., Van der Lee, T., Bleeker, M., Onstenk, J., de Both, M., Haring, M., Mes, J., Cornelissen, B., Zabeau, M., and Vos, P. (1998) Dissection of the fusarium I2 gene cluster in tomato reveals six homologs and one active gene copy. *Plant Cell* **10**, 1055-1068
40. Ma, L., Cornelissen, B. J., and Takken, F. L. (2013) A nuclear localization for Avr2 from Fusarium oxysporum is required to activate the tomato resistance protein I-2. *Front Plant Sci* **4**, 94
41. Heidrich, K., Wirthmueller, L., Tasset, C., Pouzet, C., Deslandes, L., and Parker, J. E. (2011) Arabidopsis EDS1 connects pathogen effector recognition to cell compartment-specific immune responses. *Science* **334**, 1401-1404
42. Tameling, W. I., Nooijen, C., Ludwig, N., Boter, M., Slootweg, E., Goverse, A., Shirasu, K., and Joosten, M. H. (2010) RanGAP2 mediates nucleocytoplasmic partitioning of the NB-LRR immune receptor Rx in the Solanaceae, thereby dictating Rx function. *Plant Cell* **22**, 4176-4194
43. Kelley, L. A., and Sternberg, M. J. (2009) Protein structure prediction on the Web: a case study using the Phyre server. *Nat Protoc* **4**, 363-371
44. Karplus, K. (2009) SAM-T08, HMM-based protein structure prediction. *Nucleic Acids Res* **37**, W492-497
45. Heo, L., Park, H., and Seok, C. (2013) GalaxyRefine: Protein structure refinement driven by side-chain repacking. *Nucleic Acids Res* **41**, W384-388
46. Schrodinger, LLC. (2010) The PyMOL Molecular Graphics System, Version 1.3r1.
47. Gaudier, M., Schuwirth, B. S., Westcott, S. L., and Wigley, D. B. (2007) Structural basis of DNA replication origin recognition by an ORC protein. *Science* **317**, 1213-1216
48. Green, V., Curtis, F. A., Sedelnikova, S., Rafferty, J. B., and Sharples, G. J. (2013) Mutants of phage bIL67 RuvC with enhanced Holliday junction binding selectivity and resolution symmetry. *Mol Microbiol* **89**, 1240-1258
49. Dueber, E. L., Corn, J. E., Bell, S. D., and Berger, J. M. (2007) Replication origin recognition and deformation by a heterodimeric archaeal Orc1 complex. *Science* **317**, 1210-1213
50. Clegg, R. M. (1992) Fluorescence resonance energy transfer and nucleic acids. *Methods Enzymol* **211**, 353-388
51. Grinvald, A., and Steinberg, I. Z. (1974) On the analysis of fluorescence decay kinetics by the method of least-squares. *Anal Biochem* **59**, 583-598
52. Edelman, L. M., Cheong, R., and Kahn, J. D. (2003) Fluorescence resonance energy transfer over approximately 130 basepairs in hyperstable lac repressor-DNA loops. *Biophys J* **84**, 1131-1145
53. Parkhurst, K. M., and Parkhurst, L. J. (1995) Kinetic studies by fluorescence resonance energy transfer employing a double-labeled oligonucleotide: hybridization to the oligonucleotide complement and to single-stranded DNA. *Biochemistry* **34**, 285-292
54. Vamosi, G., Gohlke, C., and Clegg, R. M. (1996) Fluorescence characteristics of 5-carboxytetramethylrhodamine linked covalently to the 5' end of oligonucleotides: multiple conformers of single-stranded and double-stranded dye-DNA complexes. *Biophys J* **71**, 972-994
55. Albrecht, M., and Takken, F. L. W. (2006) Update on the domain architectures of NLRs and R proteins. *Biochem Biophys Res Commun* **339**, 459-462
56. Van der Biezen, E. A., and Jones, J. D. (1998) Plant disease-resistance proteins and the gene-for-gene concept. *Trends Biochem Sci* **23**, 454-456

57. Sanger, F., Coulson, A. R., Friedmann, T., Air, G. M., Barrell, B. G., Brown, N. L., Fiddes, J. C., Hutchison, C. A., 3rd, Slocombe, P. M., and Smith, M. (1978) The nucleotide sequence of bacteriophage phiX174. *J Mol Biol* **125**, 225-246
58. Yokoyama, H., Kurumizaka, H., Ikawa, S., Yokoyama, S., and Shibata, T. (2003) Holliday junction binding activity of the human Rad51B protein. *J Biol Chem* **278**, 2767-2772
59. Gaudreault, M., Gingras, M.-E., Lessard, M., Leclerc, S., and Guerin, S. L. (2009) Electrophoretic mobility shift assays for the analysis of DNA-protein interactions. in *DNA-Protein Interactions: Principles and Protocols* (Moss, T., and Leblanc, B. eds.), Third Ed., Humana Press. pp 15-35
60. Grainge, I., Gaudier, M., Schuwirth, B. S., Westcott, S. L., Sandall, J., Atanassova, N., and Wigley, D. B. (2006) Biochemical analysis of a DNA replication origin in the archaeon Aeropyrum pernix. *J Mol Biol* **363**, 355-369
61. Gohlke, C., Murchie, A. I., Lilley, D. M., and Clegg, R. M. (1994) Kinking of DNA and RNA helices by bulged nucleotides observed by fluorescence resonance energy transfer. *Proc Natl Acad Sci USA* **91**, 11660-11664
62. Fujimoto, M., Kuninaka, A., and Yoshino, H. (1974) Studies on a Nuclease from Penicillium-Citrinum .1. Purification of a Nuclease from Penicillium-Citrinum. *Agr Biol Chem Tokyo* **38**, 777-783
63. Tsuda, K., and Katagiri, F. (2010) Comparing signaling mechanisms engaged in pattern-triggered and effector-triggered immunity. *Curr Opin Plant Biol* **13**, 459-465
64. Lee, D. G., Makhov, A. M., Klemm, R. D., Griffith, J. D., and Bell, S. P. (2000) Regulation of origin recognition complex conformation and ATPase activity: differential effects of single-stranded and double-stranded DNA binding. *Embo J* **19**, 4774-4782
65. Rairdan, G. J., and Moffett, P. (2006) Distinct domains in the ARC region of the potato resistance protein Rx mediate LRR binding and inhibition of activation. *Plant Cell* **18**, 2082-2093
66. Fernandez-Cid, A., Riera, A., Tognetti, S., Herrera, M. C., Samel, S., Evrin, C., Winkler, C., Gardenal, E., Uhle, S., and Speck, C. (2013) An ORC/Cdc6/MCM2-7 complex is formed in a multistep reaction to serve as a platform for MCM double-hexamer assembly. *Mol Cell* **50**, 577-588
67. Randell, J. C., Bowers, J. L., Rodriguez, H. K., and Bell, S. P. (2006) Sequential ATP hydrolysis by Cdc6 and ORC directs loading of the Mcm2-7 helicase. *Mol Cell* **21**, 29-39

Acknowledgments- We thank Wladimir Tameling for making recombinant I-2 proteins.

FOOTNOTES

* This work was supported by BBSRC grant BB/M007405/1 to MJC, GJS and LOP AND EU-funded Integrated Project BIOEXPLOIT to FLWT.

[1]School of Biological and Biomedical Sciences, [2]Biophysical Sciences Institute, [3]Department of Chemistry, Durham University, South Road, Durham, DH1 3LE, United Kingdom. [4]Molecular Plant Pathology, Swammerdam Institute for Life Sciences, University of Amsterdam, Science Park 904, 1098 XH, Amsterdam, The Netherlands. [5] These authors contributed equally to this work

[6] The abbreviations used are: AAA+, ATPases Associated with diverse cellular Activities; CC, Coiled-Coil; EMSA, Electrophoretic Mobility Shift Assays; CNL, Coiled-Coil Nucleotide-Binding Leucine-rich Repeat; FRET, Fluorescence Resonance Energy Transfer; NB, Nucleotide-Binding; NB-ARC, Nucleotide-Binding, Apaf-1, R-proteins, and CED-4; LRR, Leucine-Rich Repeat; NLR, Nucleotide-binding Leucine-rich Repeat; STAND, Signal-Transduction ATPases with Numerous Domains; TIR, Toll–Interleukin 1 Receptor.

FIGURE LEGENDS

Figure 1. The I-2 CC-NB-ARC domains bind nucleic acids *in vitro*. **A.** Structural homology model for amino acids 175-519 encompassing the NB-ARC domain of I-2, with associated ADP, bound to DNA. **B.** Proteins used in this study. The upper bar represents a generic CC-NB-LRR type R protein. Conserved domains are highlighted; CC-coiled coil; NB-ARC-nucleotide binding domain found in Apaf-1, R-protein, Ced-4; LRR-leucine rich repeat. The NB subdomain of the NB-ARC domain containing the P-loop is shown in orange and the tandem ARC subdomains are shown in cyan. The lower bars depict the domain composition of the proteins used, with amino acid positions delineating the relevant regions cloned. **C.** EMSA for I-$2_{1\text{-}519}^{WT}$ using 100 ng ΦX174 DNA (ssDNA) or ΦX174 RF I DNA (dsDNA). For dsDNA two bands are visible; the upper band represents relaxed circular DNA while the lower band represents supercoiled circular DNA, note that both bands shift in the presence of I-$2_{1\text{-}519}^{WT}$. Molecular weight markers are indicated with arrows.

Figure 2. The I-2 CC-NB-ARC domain and the R1 NB domain bind nucleic acids *in vitro*. **A.** Quantitative EMSA analysis giving affinities of I-$2_{1\text{-}519}^{WT}$ for synthetic oligonucleotides corresponding to different nucleic acids (*n*=3-6, ±S.E.M). **B.** Overlay of a structural homology model for amino acids 197-334 encompassing the NB domain of R1-NB (blue) onto the I-2 NB-ARC domain model of Figure 1A (yellow). **C.** EMSA for R1-NB using 100 ng ΦX174 DNA (ssDNA) or ΦX174 RF I DNA (dsDNA). For dsDNA the upper band represents relaxed circular DNA while the lower band represents supercoiled circular DNA, note that both bands shift upon incubation with the R1 NB domain. Molecular weight markers are indicated with arrows. **D**. Quantitative EMSA analysis giving affinities of R1 NB for various synthetic oligonucleotides corresponding to different nucleic acids (*n*=3-10, ±S.E.M).

Figure 3. The I-2 K207R mutant shows an altered mode of interaction with dsDNA in comparison with wild type I-2. **A.** Quantitative EMSA analysis giving comparative affinities of I-$2_{1\text{-}519}^{WT}$ and I-$2_{1\text{-}519}^{K207R}$ for synthetic dsDNA oligonucleotides (*n*=3, ±S.E.M). **B.** Fluorescence anisotropy analysis giving distinct affinities of I-$2_{1\text{-}519}^{WT}$ and I-$2_{1\text{-}519}^{K207R}$ for dsDNA (*n*=3, ±S.E.M) suggestive for a different topology of the protein-DNA complex.

Figure 4. I-$2_{1\text{-}519}$ distorts and melts dsDNA. **A.** Energy transfer efficiency in steady-state FRET in response to I-$2_{1\text{-}519}$ binding (*n*=3, ±S.E.M.). The control is BSA. **B.** Energy transfer efficiency in time resolved FRET in response to I-$2_{1\text{-}519}$ binding. **C.** P_1 nuclease sensitivity of ssDNA and dsDNA following incubation with BSA (negative control), I-$2_{1\text{-}519}$ or ORC (positive control). * $p<0.01$ compared to control by one-way ANOVA with post-hoc Dunnett test.

Figure 5. DNA binding is coupled to the nucleotide binding state and ATPase activity of I-$2_{1\text{-}519}$. **A.** The influence of 2 μM DNA on the intrinsic ATPase activity of I-$2_{1\text{-}519}^{WT}$ and I-$2_{1\text{-}519}^{K207R}$ (* $p<0.05$, # $p>0.05$, *n*=4, ±S.E.M). The source DNA is identical to that used for EMSA in Figure 2A **B.** Double-stranded DNA binding by I-$2_{1\text{-}519}^{WT}$ and I-$2_{1\text{-}519}^{K207R}$ assessed by EMSA plotted as a ratio of binding in the presence of 5 μM nucleotide (ADP, ATP or β, γ-imido ATP) compared with no nucleotide (* $p<0.05$, # $p>0.05$, *n*=4-6, ±S.E.M). **C.** Quantitative EMSA analysis giving comparative affinities of I-$2_{1\text{-}519}^{WT}$ and I-$2_{1\text{-}519}^{S233F}$ for synthetic dsDNA oligonucleotides (*n*=3, ±S.E.M).

TABLE 1 Apparent dissociation constants for recombinant NLR domain interactions with nucleic acids. Error values represent the standard deviation.

Protein	**Method**	K_d **ssDNA [μM]**	K_d **dsDNA [μM]**	K_d **ssRNA [μM]**
$I\text{-}2_{1\text{-}519}^{WT}$	EMSA	0.15±0.01	0.22±0.02	>100
$I\text{-}2_{1\text{-}519}^{K207R}$	EMSA	ND	0.23±0.01	ND
$I\text{-}2_{1\text{-}519}^{WT}$	Anisotropy	ND	0.32±0.05	ND
$I\text{-}2_{1\text{-}519}^{K207R}$	Anisotropy	ND	0.94±0.09	ND
R1-NB	EMSA	3.34±0.54	2.75±0.40	12.45±2.34

Figure 1

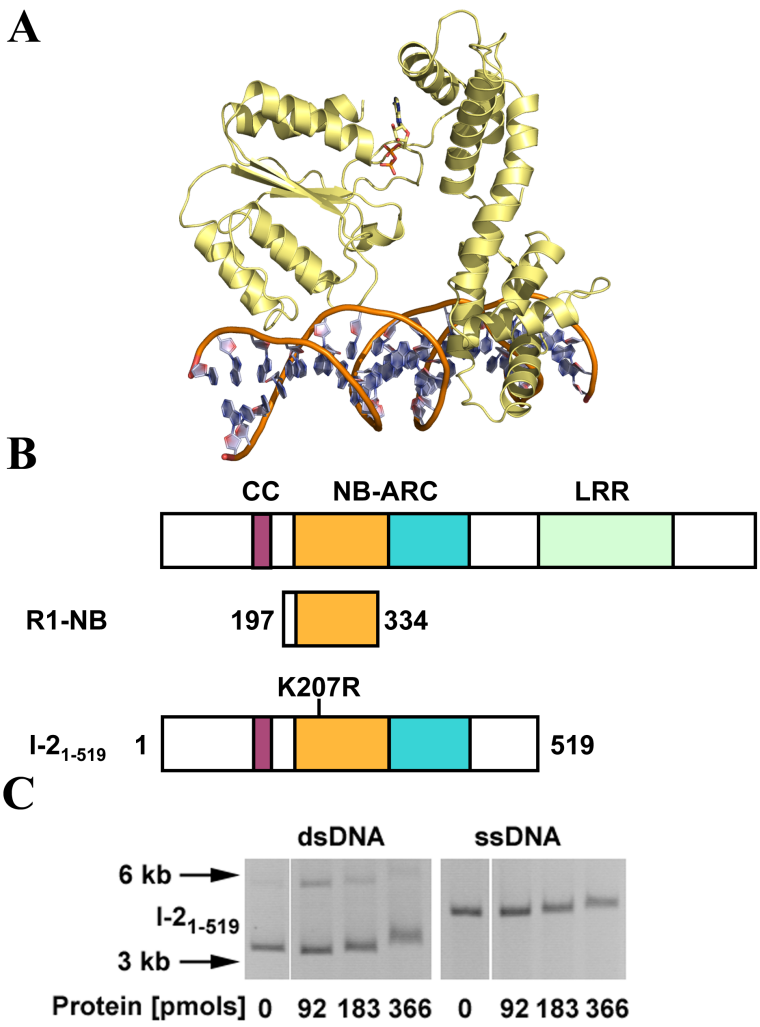
A
B
CC
NB-ARC
LRR
R1-NB
197
334
K207R
I-2$_{1-519}$
1
519
C
dsDNA
ssDNA
6 kb
I-2$_{1-519}$
3 kb
Protein [pmols] 0 92 183 366 0 92 183 366

Figure 2

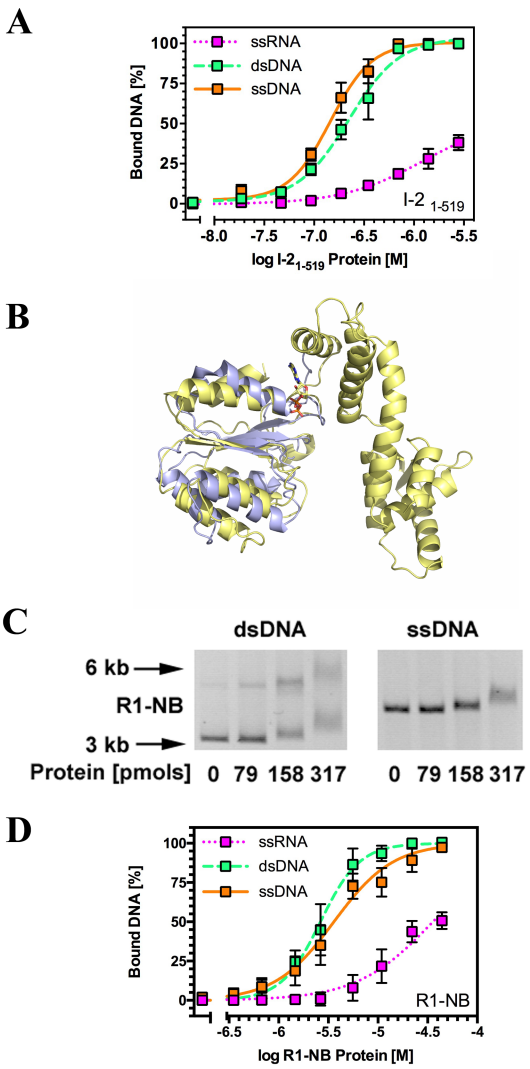
A
ssRNA
dsDNA
ssDNA
Bound DNA [%]
I-2 1-519
log I-2 1-519 Protein [M]
B
C
dsDNA
ssDNA
6 kb
R1-NB
3 kb
Protein [pmols] 0 79 158 317 0 79 158 317
D
ssRNA
dsDNA
ssDNA
Bound DNA [%]
R1-NB
log R1-NB Protein [M]

Figure 3

A

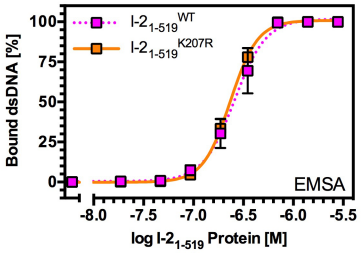
I-2 1-519 WT
I-2 1-519 K207R
Bound dsDNA [%]
100
75
50
25
0
EMSA
-8.0
-7.5
-7.0
-6.5
-6.0
-5.5
log I-2 1-519 Protein [M]

B

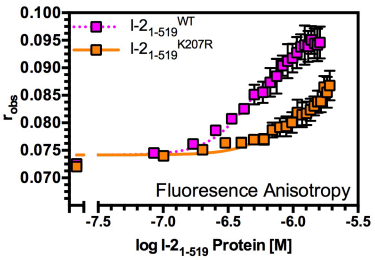
I-2 1-519 WT
I-2 1-519 K207R
r obs
0.100
0.095
0.090
0.085
0.080
0.075
0.070
Fluoresence Anisotropy
-7.5
-7.0
-6.5
-6.0
-5.5
log I-2 1-519 Protein [M]

Figure 4

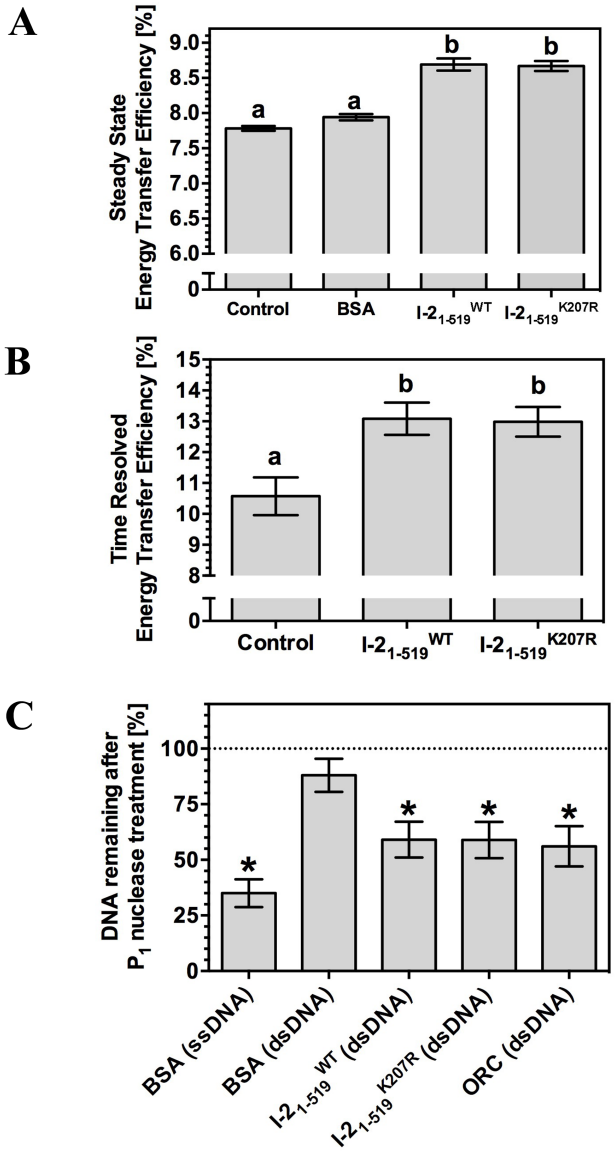
A
Steady State Energy Transfer Efficiency [%]
9.0
8.5
8.0
7.5
7.0
6.5
6.0
0
a
a
b
b
Control
BSA
I-2 1-519 WT
I-2 1-519 K207R
B
Time Resolved Energy Transfer Efficiency [%]
15
14
13
12
11
10
9
8
0
a
b
b
Control
I-2 1-519 WT
I-2 1-519 K207R
C
DNA remaining after P1 nuclease treatment [%]
100
75
50
25
0
*
*
*
*
BSA (ssDNA)
BSA (dsDNA)
I-2 1-519 WT (dsDNA)
I-2 1-519 K207R (dsDNA)
ORC (dsDNA)

Figure 5

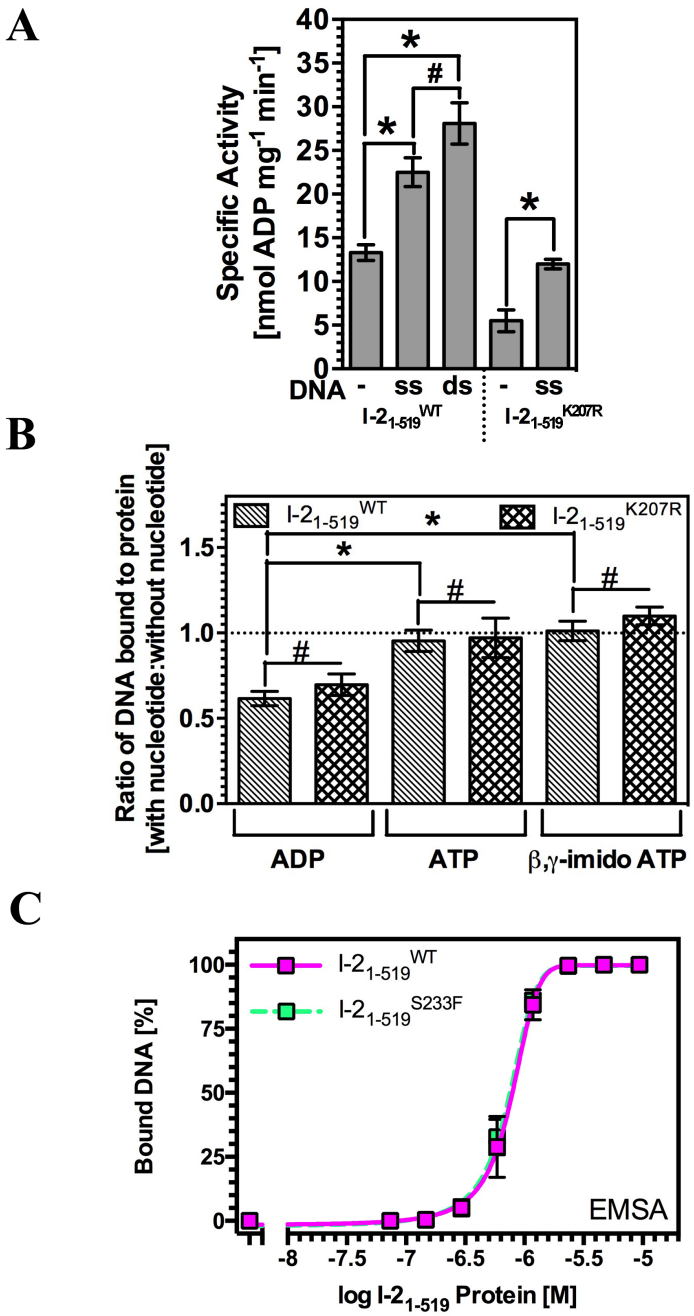
A
Specific Activity [nmol ADP mg-1 min-1]
DNA - ss ds - ss
I-21-519WT
I-21-519K207R
B
Ratio of DNA bound to protein [with nucleotide:without nucleotide]
I-21-519WT
I-21-519K207R
ADP
ATP
β,γ-imido ATP
C
Bound DNA [%]
I-21-519WT
I-21-519S233F
EMSA
log I-21-519 Protein [M]